

# Global water cycle agreement in the climate models assessed in the IPCC AR4

D. Waliser,<sup>1</sup> K.-W. Seo,<sup>1</sup> S. Schubert,<sup>2</sup> and E. Njoku<sup>1</sup>

Received 22 May 2007; revised 27 June 2007; accepted 9 July 2007; published 18 August 2007.

[1] This study examines the fidelity of the global water cycle in the climate model simulations assessed in the IPCC Fourth Assessment Report. The results demonstrate good model agreement in quantities that have had a robust global observational basis and that are physically unambiguous. The worst agreement occurs for quantities that have both poor observational constraints and whose model representations can be physically ambiguous. In addition, components involving water vapor (frozen water) typically exhibit the best (worst) agreement, and fluxes typically exhibit better agreement than reservoirs. These results are discussed in relation to the importance of obtaining accurate model representation of the water cycle and its role in climate change. Recommendations are also given for facilitating the needed model improvements.  
**Citation:** Waliser, D., K.-W. Seo, S. Schubert, and E. Njoku (2007), Global water cycle agreement in the climate models assessed in the IPCC AR4, *Geophys. Res. Lett.*, **34**, L16705, doi:10.1029/2007GL030675.

## 1. Introduction

[2] Two recent studies have provided estimates of the global water cycle (GWC) based on up to date observational resources [Oki and Kanae, 2006; Trenberth *et al.*, 2007]. These studies join only a few that have even attempted to characterize and quantify the GWC in a comprehensive manner [e.g., Chahine, 1992; Oki, 1999]. Their estimates include leading quantities that typically have a relatively sound observational basis, such as the ocean water mass, atmospheric water vapor, precipitation and runoff. In addition, there are attempts by the authors to also ascertain more obscure quantities that are often relatively small and/or have a more tenuous observational foundation, such as ground-water, river and lake storage, biological storage, snowfall, and subsurface runoff. The convergence in values among these studies of some of the leading quantities [cf. Schlosser and Houser, 2007] suggests that the global characterization of the water cycle is nearing a robust enough stage to assess climate models. In particular, it is important to quantify how well the global atmosphere-ocean coupled climate models (AOGCMs) assessed in the Fourth Assessment Report (AR4) [Intergovernmental Panel on Climate Change, 2007] by the Intergovernmental Panel on Climate Change (IPCC) represent the GWC since the most important climate feedbacks under a scenario of increasing greenhouse gases

(GHGs) are inherently related to the water cycle. This includes the water vapor, cloud, sea-ice and snow-albedo feedbacks. Apart from this, there are stark changes projected for a number of socially-relevant and environmentally-important components of water cycle, particularly on a regional scale, including soil moisture, rainfall, snowpack, and sea-ice [e.g., Trenberth *et al.*, 2003]. Both these considerations warrant close examination of the fidelity of such models to represent the totality of the GWC.

[3] There have been numerous studies examining the representation and climate projections of various components of the GWC in AOGCMs. This includes studies of precipitation, evaporation minus precipitation, atmospheric water vapor and its transport, sea-ice, and soil moisture [e.g., Milly *et al.*, 2002; Hirabayashi *et al.*, 2005; Lambert *et al.*, 2005]. However, there have been few studies that have examined this in a comprehensive manner in terms of a wide range of water cycle components, including those in the atmosphere, over land, and the cryosphere. In this study, we examine the fidelity of AOGCMs assessed in the AR4 in representing the GWC. This is performed mainly in terms of analysis of model-to-model agreement and in a few cases against observations where they are available and robust. The model-to-model agreement is examined with respect to the models' representations of the 20th century climate as well as their agreement under an increasing GHG scenario.

## 2. Models and observations

[4] The model output is based on the WCRP CMIP3 multi-model archive at PCMDI from simulations of 20th century conditions and those from an increasing GHG scenario (i.e. rising to  $\sim 2.5$  times pre-industrial  $\text{CO}_2$ ), referred to as SRES A1B [Meehl *et al.*, 2007]. The period used for the former is 1970–1994, while that for the latter is 2070–2094. While the AR4 database does not include a number of components of the GWC (e.g., ground-water, biological water, lake and river storage), this analysis includes nearly all available variables that are directly associated with the GWC. In all cases, the data have been globally and time averaged. Note that runoff contributions are only those from land. For those models that provide more than one ensemble member for the given century/scenario, only the first is utilized.

## 3. Results

### 3.1. Comparison to Observations

[5] Figure 1 shows the model-to-model and model-to-data agreements for a few fundamental quantities associated with the GWC. For all but snow mass, the observed value is shown in the far right portion of the plot. Evident is the relatively good agreement for precipitation and precipitable

<sup>1</sup>Water and Carbon Cycles Group, Jet Propulsion Laboratory, Pasadena, California, USA.

<sup>2</sup>Global Modeling and Assimilation Office, NASA Goddard Space Flight Center, Greenbelt, Maryland, USA.

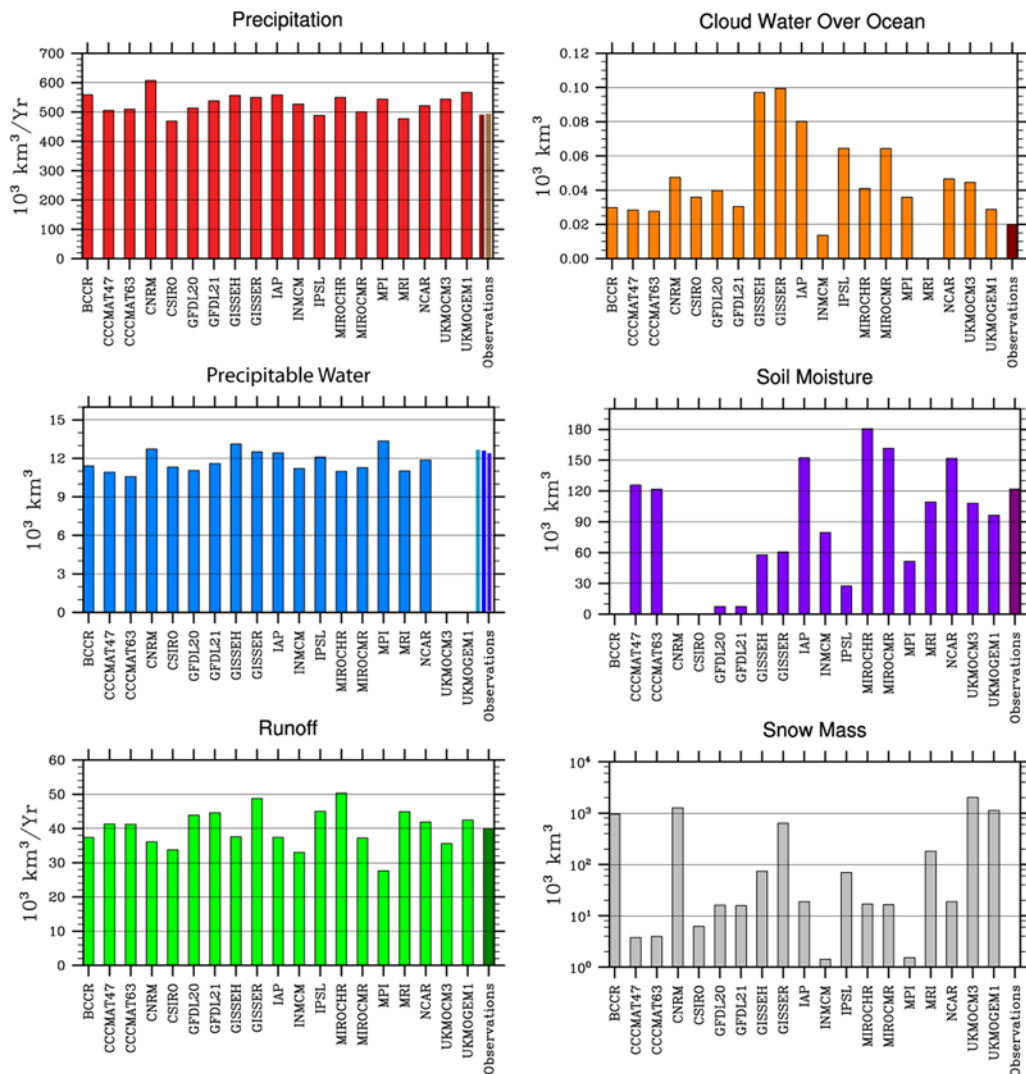


**Figure 1.** Globally-averaged, annual mean values of hydrological quantities from the 1970–1994 period of the 20th century AOGCM simulations assessed in the IPCC AR4. Observed values are given for all but snow mass (lower right). The observed values for runoff and soil moisture are from *Trenberth et al.* [2007]; precipitation from GPCP (left thin bar) [Huffman et al., 1997] and CMAP (right thin bar) [Xie and Arkin, 1997]; precipitable water from NCEP/NCAR (left thin bar) [Kalnay et al., 1996], NVAP (middle thin bar) [Randel et al., 1996], and ERA40 (right thin bar) [Trenberth and Smith, 2005]; and cloud water over the ocean from SSM/I satellite-based estimates [Weng et al., 1997]. Zero values indicate that the given model did not provide this variable to the CMIP3 database.

water. While it is understood that there exist large discrepancies in these quantities between models on a regional scale [e.g., Waliser et al., 2003], the representation of their globally-averaged values is quite good. This stems from the long-standing observational constraints that have been available for these quantities as well as indirect constraints from well-measured energy cycle quantities (e.g., top of the atmosphere energy balance). Another aspect that leads to their good agreement, in contrast to some quantities discussed below, is that there is no ambiguity in terms of the physical nature of the quantity being represented.

[6] Exhibiting poorer model agreements are runoff and (over ocean) cloud water content. For these quantities, not only is the physical process arguably more complex to model correctly but the observational foundation is more challenging. For example, runoff is largely based only on measurements from river gauges – which have limitations

[Dai and Trenberth, 2002; Alsdorf and Lettenmaier, 2003] – and in some cases through indirect residual calculations that rely on quantities that have considerable uncertainty (e.g., evapotranspiration, water vapor transport). In the case of cloud water, the observations to date have simply been too indirect (i.e. remotely sensed), experimental or too sparse (i.e. in-situ) to provide a robust AOGCM constraint [e.g., Horváth and Davies, 2007]. Thus, the greater model disagreement in cloud water, over for example precipitable water, is not only due to the challenge of the modeling clouds [Jakob, 2003; Randall et al., 2003] but also because the observational constraints have lacked robustness and/or been insufficiently defined which leaves models significant leeway in their representation.

[7] Finally, Figure 1 shows that the AOGCMs contributing to the AR4 exhibit very poor agreement in soil moisture and snow mass. This level of disagreement stems not only

from the complex nature of the process being modeled and the lack of robust direct measurements on a global scale, as discussed above with runoff and cloud water, but also due to the fact that the models are inherently representing these quantities differently. For example, not all models attempt to model the total soil moisture but rather only that in the uppermost meter or so, and in some cases this is done quite differently [Koster and Milly, 1997; Dirmeyer et al., 2006; R. Koster et al., A common misinterpretation of model-generated soil moisture, unpublished report, GEWEX/GLASS Panel, 2007]. A similar ambiguity holds for snow mass, including the accounting for glaciers [Frei and Gong, 2005; Roesch, 2006]. While it is arguable then whether it is appropriate to compare them given the different approaches made by the different modeling groups, there is still good reason to be concerned with these levels of disagreement. Soil moisture, and snow mass in particular, represent very important water reservoirs, both physically to the climate system as well as to society. These reservoirs play a key role in the manifestations of their associated climate feedbacks. For example, how much could the level of disagreement in globally-averaged warming projections be reduced if AOGCMs were more consistent in modeling at least the physical structure (e.g., depths or masses) of the water cycle? In addition, these AOGCM-based simulations are used to project the impacts of global change on future water availability. In this regard, it is crucial that the models provide a physically meaningful and consistent representation.

### 3.2. Uncertainty in Water Cycle Simulations

[8] Figure 2 shows a measure of agreement among the models for all the water cycle components considered in this study. Each bar on the plot represents a measure of the model agreement in the globally-averaged, long-term (i.e. 25 years) mean value for the given variable. From the distribution of modeled values,  $M$ , the mean model value is computed, and is denoted here as  $\bar{M}$ . Then the deviation, in terms of percent, of each model's value is computed as  $M' = 100\% * (M - \bar{M}) / \bar{M}$ . The box plots in Figure 2 show the maximum and minimum  $M'$  values (as the ends of the "error" bars) and the standard deviation of the  $M'$  values (as the box that extends about zero). The variables are plotted from left to right according to the size of these standard deviations. Looking at Figure 2 (bottom), it can be seen more clearly that the model agreement for globally-averaged precipitation, evaporation, and precipitable water is about 10%. On the other hand, for variables at the other extreme such as snow mass and snow depth, the level of agreement is on the order of 200%.

[9] The additional notation on Figure 2 indicates whether the given quantity is a flux (red) or a reservoir (blue) and what state(s) of water are involved. For example, precipitable water is a reservoir, the label is blue, and the molecule icon indicates the vapor state. Snowmelt is a flux, the label is red, and the icons indicate transformations between the frozen and liquid states, shown as a snowflake and water droplet, respectively. From this information, the following conclusions can be drawn. First, models demonstrate better agreement at representing the fluxes than the reservoirs. To a great degree the agreement in the former, particularly evaporation, precipitation and to some extent runoff, is due

to having relatively good observational constraints of the given quantity but also from additional physical constraints and observations associated with the connections between the energy (e.g., top-of-the-atmosphere fluxes) and water cycles. The relatively poorer agreement in the reservoir terms, for all but precipitable water, is due to the much poorer observational foundation for these quantities and the issue raised above regarding the differences in the manner/amount of these reservoirs being represented in the models. Second, models demonstrate considerably better levels of agreement with the vapor and liquid components of the water cycle than the frozen ones. Keep in mind the situation is a bit exaggerated here because there are three measures of snow (depth, mass and cover) and two measures of sea ice (fraction, thickness). However, even if only one of the sea ice and snow measures were used, the conclusion would remain the same.

### 3.3. Uncertainty in Projected Changes to the Water Cycle

[10] Figure 3 illustrates the level of agreement in the model-projected changes between the decades 1970–1989 to 2070–2089. In Figure 3 (top), each model's change is normalized by its own 20th century globally-averaged annual mean value, referred to here as  $M_{20}$ . Similar to Figure 2, the box plots in Figure 3 (top) represent the statistics (i.e. maximum, minimum and standard deviation) associated with the distribution of model changes calculated from:  $100\% * (M_{21} - M_{20}) / M_{20}$ . In this case, the order from left to right is the same as that for Figure 2. To some degree, the uncertainty associated with the model projected changes mimics that from the model uncertainty associated with the 20th century simulations. Meaning, the more uncertain a given variable is across models – as shown in Figure 2, the more uncertain are its changes. However, this is not strictly the case; uncertainty in changes in snowcover, soil moisture and cloud ice are small relative to the uncertainty level in simulating their present-day global averages. Changes in global mean evaporation and precipitation exhibit relatively good agreement, while those for example for snow and sea ice exhibit rather poor agreement.

[11] Blue labels on the plot in Figure 3 indicate changes in quantities that suggest an enhancement to the atmospheric component of the hydrological cycle. This includes rather robust model agreement in terms of positive changes to precipitation, evaporation, precipitable water and runoff. Red labels on the plot (subjectively) indicate important climate feedback quantities that display considerable uncertainty, either in terms of lacking a consistent sign in the projected change or by simply having a relatively large uncertainty ( $>20\text{--}30\%$ ). The latter include sea ice quantities and frozen soil moisture, while the former includes cloud variables, soil moisture and snow quantities. For example, the range of reduction to sea-ice thickness is between  $-30$  to  $-75\%$ , and for snow depth  $+20$  to  $-30\%$ . While the uncertainty in cloud ice and water shown here isn't a direct measure of the radiative component of cloud feedback, it does illustrate the uncertainty in terms of the impact on the GWC, that at this point is still uncertain in sign.

[12] Figure 3 (bottom) shows similar information as Figure 3 (top) but in this case each model's changes are normalized by its globally-averaged annual mean surface air

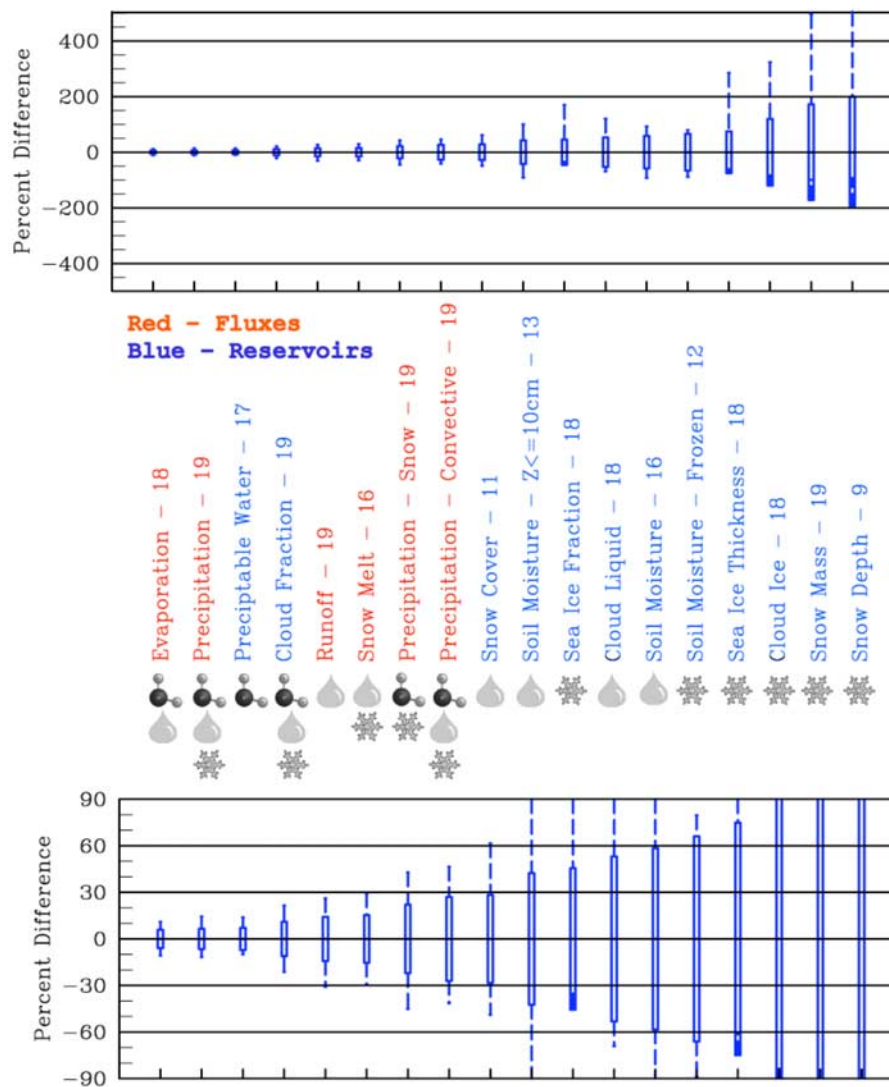


**Figure 2.** (top) Model-to-model agreement in globally-averaged, annual mean values of hydrological quantities from 1970–1994 of the 20th century AOGCM simulations assessed in the IPCC AR4. Quantities are ordered in increasing model disagreement using the standard deviation (see text for details). (bottom) Same as for Figure 2 (top), except for expanded y-scale. Horizontal labels consist of the variable name and the number of model contributions included. Font color indicates whether the water cycle component is a flux (red) or reservoir (blue). In addition, model variables are labeled with icons indicating whether the variable is associated with vapor (molecule), liquid (drop), and/or ice (snowflake).

temperature change between the 20th and 21st centuries ( $\Delta T$ ). Thus in this case, the distribution of modeled changes is calculated from:  $100\% * (M_{21} - M_{20}) / (M_{20} * \Delta T)$ . In addition, the variables are displayed from left to right in terms of the standard deviation of this distribution – rather than that used in the upper panel (i.e. the order calculated and used in Figure 2). Thus, the variables whose relative change from the 20th to the 21st century exhibit good (poor) model agreement are on the left (right). Finally, the same icons used in Figure 2 are added to the labels to indicate which phases of water are involved. From Figure 3, it is still fairly evident that agreement in modeled projected changes of the frozen components of the water cycle is poorer than for the modeled projected changes of the vapor and liquid components. In addition, there is still a tendency for better model agreement in fluxes than reservoirs, although it is not

as dramatic as for the model agreement of 20th century climate.

#### 4. Summary

[13] This study examines the fidelity of the global water cycle in the climate model simulations assessed in the IPCC Fourth Assessment Report. The results demonstrate rather good agreement in 20th century climate representations of quantities that have a relatively robust global observational basis and that are physically unambiguous (e.g., rainfall, precipitable water). Poorer agreement occurs for quantities that have a weak or still uncertain global observational basis (e.g., snow fall, cloud liquid) or that can be physically ambiguous with respect to model representation (e.g., soil moisture, snow mass). The worst agreement tends to occur for quantities that have both poor observational constraints and whose model representa-

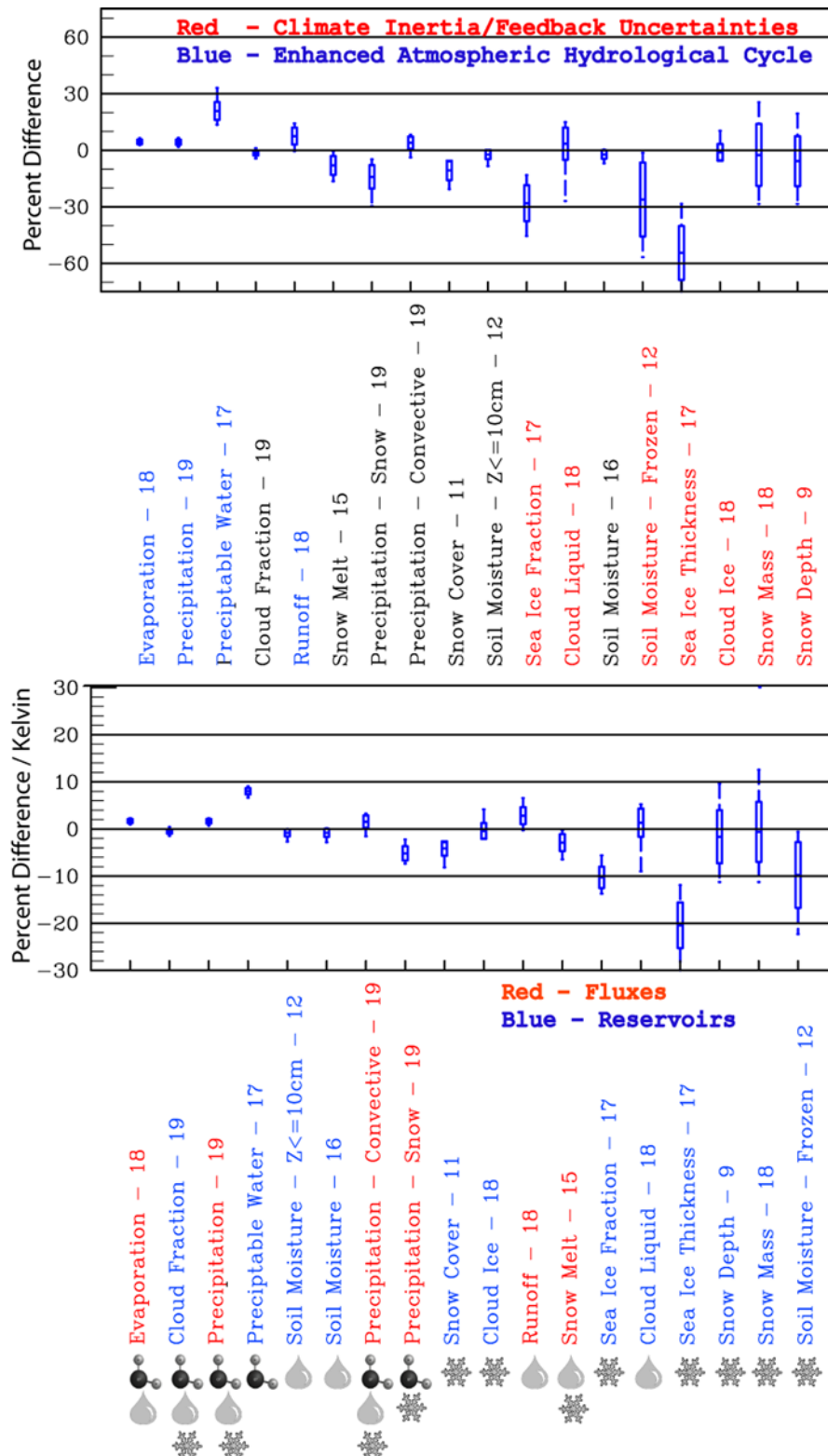


**Figure 3.** (top) Similar to Figure 2, except for the change in the values associated with an increasing GHG scenario (20th versus the 21st century). Quantities are ordered from left to right according to Figure 2 (see text for details). (bottom) Same as for Figure 3 (top), except that each modeled change is normalized by the associated globally-averaged, mean annual surface air temperature increase and the order from left to right is based on the standard deviation of the model projected changes for each variable. Annotations and icons are same as in Figure 2.

tions can be physically ambiguous (e.g., soil moisture, snow depth/mass). In addition, components involving water vapor (frozen water) typically exhibit the best (worst) model-to-model agreement, and fluxes typically exhibit better model-to-model agreement than reservoirs.

[14] For the most part, the above findings and trends also hold true for the model-projected changes in the GWC, although there are a few exceptions. While the model agreement in soil moisture and near-surface soil moisture was relatively poor when considering the 20th century representation, the agreement in their projected changes is quite good. This echoes the fact that AOGCMs represent some quantities in physically different ways. Thus, comparing such quantities from different models directly can lead to a large disagreement but when comparing their relative changes under a climate change scenario can lead to better agreement since each model's absolute value is compared only to itself. A similar behavior is exhibited by cloud ice, except that while the agreement in total cloud ice change is good (a few % per degree of warming), the modeled changes do not agree on the sign of the change. The opposite behavior is exhibited by runoff, snowmelt and frozen soil moisture, whereby the relative model agreement (in terms of variable ranking – Figure 2 vs. Figure 3) was considerably worse for the climate change than for the 20th century. This would seem to indicate that these processes are particularly sensitive to the modeled climate system and influencing feedbacks. The findings also indicate that the global atmospheric hydrological cycle will become enhanced in the 21st century via greater precipitation (5%), evaporation (5%), runoff (10%) and precipitable water (20%). Finally, the results illustrate that climate projections contain considerable uncertainty due to poor/inconsistent AOGCM representations of key climate feedbacks – including sea ice, cloud ice and water, snow depth and mass.

[15] Rectifying the above uncertainties will require more effort to model the key water cycle components, particularly reservoirs, in physically consistent ways so that they can be better compared amongst themselves and to available observations. Moreover, new measurement strategies and platforms are needed to provide constraints on a number of poorly constrained water cycle properties (e.g., soil moisture, cloud ice, sea-ice thickness, snow fall, snow mass/depth, cloud liquid). A subset of these was given high priority in the recent National Research Council Decadal study [National Research Council, 2007]. Finally, to provide a more comprehensive study of these issues, more complete representations and/or output of the GWC are needed for the next IPCC study (e.g., evapotranspiration, water vapor transport, sea-ice mass).

[16] **Acknowledgments.** Support provided by JPL's HRD Fund, the NASA NEWS and Modeling, Analysis and Prediction Programs, and the NASA Postdoctoral Program. We thank K. Trenberth and J. Meehl for a number of helpful comments. The research described in this paper was carried out at the Jet Propulsion Laboratory, Caltech, under a contract with NASA. We acknowledge the modeling groups for making their simulations available, PCMDI for collecting and archiving CMIP3, WCRP's Working Group on Coupled Modeling for organizing the analysis, and the Office of Science, U.S. Department of Energy for supporting the CMIP3 dataset.

## References

Alsdorf, D. E., and D. P. Lettenmaier (2003), Tracking fresh water from space, *Science*, 301(5639), 1491–1494.

- Chahine, M. T. (1992), The hydrological cycle and its influence on climate, *Nature*, 359(6394), 373–380.
- Dai, A. G., and K. E. Trenberth (2002), Estimates of freshwater discharge from continents: Latitudinal and seasonal variations, *J. Hydrometeorol.*, 3(6), 660–687.
- Dimmeyer, P. A., X. A. Gao, M. Zhao, Z. Guo, T. Oki, and N. Hanasaki (2006), GSWP-2: Multimodel analysis and implications for our perception of the land surface, *Bull. Am. Meteorol. Soc.*, 87(10), 1381–1397.
- Frei, A., and G. Gong (2005), Decadal to century scale trends in North American snow extent in coupled atmosphere-ocean general circulation models, *Geophys. Res. Lett.*, 32, L18502, doi:10.1029/2005GL023394.
- Hirabayashi, Y., S. Kanae, I. Struthers, and T. Oki (2005), A 100-year (1901–2000) global retrospective estimation of the terrestrial water cycle, *J. Geophys. Res.*, 110, D19101, doi:10.1029/2004JD005492.
- Horvath, A., and R. Davies (2007), Comparison of microwave and optical cloud water path estimates from TMI, MODIS, and MISR, *J. Geophys. Res.*, 112, D01202, doi:10.1029/2006JD007101.
- Huffman, G. J., R. F. Adler, P. Arkin, A. Chang, R. Ferraro, A. Gruber, J. Janowiak, A. McNab, B. Rudolf, and U. Schneide (1997), The Global Precipitation Climatology Project (GPCP) combined precipitation dataset, *Bull. Am. Meteorol. Soc.*, 78(1), 5–20.
- Intergovernmental Panel on Climate Change (2007), Climate change 2007: The physical science basis, summary for policymakers, IPCC Sec., Geneva, Switzerland.
- Jakob, C. (2003), An improved strategy for the evaluation of cloud parameterizations in GCMs, *Bull. Am. Meteorol. Soc.*, 84(10), 1387–1401.
- Kalnay, E., et al. (1996), The NCEP/NCAR 40-year reanalysis project, *Bull. Am. Meteorol. Soc.*, 77(3), 437–471.
- Koster, R. D., and P. C. D. Milly (1997), The interplay between transpiration and runoff formulations in land surface schemes used with atmospheric models, *J. Clim.*, 10(7), 1578–1591.
- Lambert, F. H., N. P. Gillett, D. A. Stone, and C. Huntingford (2005), Attribution studies of observed land precipitation changes with nine coupled models, *Geophys. Res. Lett.*, 32, L18704, doi:10.1029/2005GL023654.
- Meehl, G. A., et al. (2007), The WCRP CMIP3 multi-model dataset: A new era in climate change research, *Bull. Am. Meteorol. Soc.*, in press.
- Milly, P. C. D., et al. (2002), Increasing risk of great floods in a changing climate, *Nature*, 415(6871), 514–517.
- National Research Council (2007), *Earth Science and Applications from Space: National Imperatives for the Next Decade and Beyond*, Natl. Acad. Press, Washington, D. C.
- Oki, T. (1999), The global water cycle, in *Global Energy and Water Cycles*, edited by K. A. Browning and R. J. Gurney, pp. 292, Cambridge Univ. Press, New York.
- Oki, T., and S. Kanae (2006), Global hydrological cycles and world water resources, *Science*, 313(5790), 1068–1072.
- Randall, D., M. Khairoutdinov, A. Arakawa, and W. Grabowski (2003), Breaking the cloud parameterization deadlock, *Bull. Am. Meteorol. Soc.*, 84(11), 1547–1564.
- Randel, D. L., et al. (1996), A new global water vapor dataset, *Bull. Am. Meteorol. Soc.*, 77(6), 1233–1246.
- Roesch, A. (2006), Evaluation of surface albedo and snow cover in AR4 coupled climate models, *J. Geophys. Res.*, 111, D15111, doi:10.1029/2005JD006473.
- Schlusser, C. A., and P. Houser (2007), Assessing a satellite-era perspective of the global water cycle, *J. Clim.*, 20(7), 1316–1338.
- Trenberth, K. E., and L. Smith (2005), The mass of the atmosphere: A constraint on global analyses, *J. Clim.*, 18(6), 864–875.
- Trenberth, K. E., A. Dai, R. M. Rasmussen, and D. B. Parsons (2003), The changing character of precipitation, *Bull. Am. Meteorol. Soc.*, 84(9), 1205–1217.
- Trenberth, K. E., et al. (2007), Estimates of the global water budget and its annual cycle using observational and model data, *J. Hydrometeorol.*, in press.
- Waliser, D. E., et al. (2003), AGCM simulations of intraseasonal variability associated with the Asian summer monsoon, *Clim. Dyn.*, 21, 423–446.
- Weng, F. Z., et al. (1997), Cloud liquid water climatology from the special sensor microwave/imager, *J. Clim.*, 10(5), 1086–1098.
- Xie, P. P., and P. A. Arkin (1997), Global precipitation: A 17-year monthly analysis based on gauge observations, satellite estimates, and numerical model outputs, *Bull. Am. Meteorol. Soc.*, 78(11), 2539–2558.

E. Njoku, K.-W. Seo, and D. Waliser, Water and Carbon Cycles Group, Jet Propulsion Laboratory, 4800 Oak Grove Drive, MS 183-501, Pasadena, CA 91109, USA. (waliser@caltech.edu)

S. Schubert, Global Modeling and Assimilation Office, NASA Goddard Space Flight Center, Code 910.3, Greenbelt, MD 20771, USA.